Eur. Phys. J. A (2022) 58:235
https://doi.org/10.1140/epja/s10050-022-00883-8

THE EUROPEAN PHYSICAL JOURNAL A

Review

^{99}Tc in stars, reactors, and nuclear medicine

Yasuki Nagai[1,2,3,a], **Masayuki Igashira**[4,b]

[1] Department of Physics, Tokyo Institute of Technology, O-Okayama, Meguro, Tokyo 152-8550, Japan
[2] Research Center for Nuclear Physics, Osaka University, Ibaraki, Osaka 567-0047, Japan
[3] Quantum Beam Science Research Directorate, National Institutes for Quantum and Radiological Science and Technology, Tokai, Ibaraki 319-1106, Japan
[4] Research Laboratory for Nuclear Reactors, Tokyo Institute of Technology, O-Okayama, Meguro, Tokyo 152-8550, Japan

Received: 9 August 2022 / Accepted: 31 October 2022

Communicated by Nicolas Alamanos.

Abstract The roles of ^{99g}Tc in stars and in nuclear fission reactors and that of ^{99m}Tc in nuclear medicine that were studied using neutrons provided from accelerators are reported. In addition to the critical role of ^{99g}Tc in stars, we also describe the roles of related light nuclei such as ^{16}O, and experimental studies on keV-neutron capture cross sections of these light nuclei that were performed using keV neutrons provided from a 3.2-MV Pelletron accelerator are reported. The keV-neutron capture cross section of ^{99g}Tc, that is important in studies on the nucleosynthesis of ^{99}Tc in stars and on the nuclear transmutation of long-lived nuclear wastes produced in fission reactors, were measured. The cross sections of both light nuclei and ^{99g}Tc were measured using a neutron time-of-flight method with a ns-pulsed neutron source from the ^{7}Li(p,n)^{7}Be reaction and with an anti-Compton γ-ray NaI(Tl) spectrometer. The measurements reported here were compared with the values of recent worldwide evaluated nuclear data libraries.

We proposed a method of producing ^{99m}Tc from the ^{100}Mo(n,$2n$)^{99}Mo reaction, and performed a ^{99m}Tc production experiment using a ^{nat}Mo sample and MeV neutrons from the ^{nat}C(d,n) reaction by 40 MeV deuterons at a cyclotron. Calculations for the ^{99m}Tc production with an enriched ^{100}Mo sample were also performed, and calculated results were compared with the experimental results. Moreover, the thermoseparation of ^{99m}Tc from ^{99}Mo was discussed. As a result, it was shown that ^{99m}Tc prepared by the thermoseparation using ^{99}Mo produced by the ^{100}Mo(n,$2n$)^{99}Mo reaction can be a promising substitute for the fission product ^{99}Mo.

[a] e-mail: nagai@rcnp.osaka-u.ac.jp(corresponding author)
[b] e-mail: masayuki.igashira@gmail.com

1 Introduction

Technetium (Tc) is one of two elements with an atomic number less than 83 that have no stable isotopes. In 1937, Perrier and Segré discovered Tc in a sample obtained by bombarding a Mo sample with deuterons in the 37-inch cyclotron of the Berkeley Radiation Laboratory [1]. They asked Lawrence, who invented a cyclotron in 1929 [2], to do the bombardment. In 1938, Segré and Seaborg discovered the metastable state of ^{99}Tc (^{99m}Tc) [3]. A partial decay scheme of ^{99}Mo ($T_{1/2} = 66$ h) to excited states in ^{99}Tc currently proposed is shown in Fig. 1. [4].

In 1952, Merrill discovered Tc, presumably ^{99}Tc, at the surface of red giant stars [5]. The observation of Tc provided the first powerful evidence that Tc has been synthesized recently within stars and contributed to our understanding of the origins of elements heavier than iron observed in stars [6]. Since then, the spectral observations of peculiar red giants turned out to be a prolific source of information on s-processes during the He burning stage of stellar evolution [7]. As for ^{99g}Tc, it is one of long-lived fission products (LLFPs) produced in fission reactors. LLFPs will remain as radioactive wastes for a long period if they are not transmuted into stable or short-lived nuclides. From this viewpoint, recently, much interest is paid to the nuclear transmutation studies, for which the neutron capture cross sections of individual LLFPs are the most important physical quantities. Since both the fission yield and hazard index of ^{99g}Tc are large, ^{99g}Tc is one of the most important LLFPs and its neutron capture cross section is very important.

On the other hand, among the medical radioisotopes (RIs), ^{99m}Tc ($T_{1/2} = 6$ h), the decay product of ^{99}Mo ($T_{1/2} = 66$ h), is the most widely used diagnostic nuclear medicine RI [8] that is usually obtained from a ^{99}Mo/^{99m}Tc generator. Because of the short half-life of ^{99}Mo, a constant supply

Published online: 30 November 2022

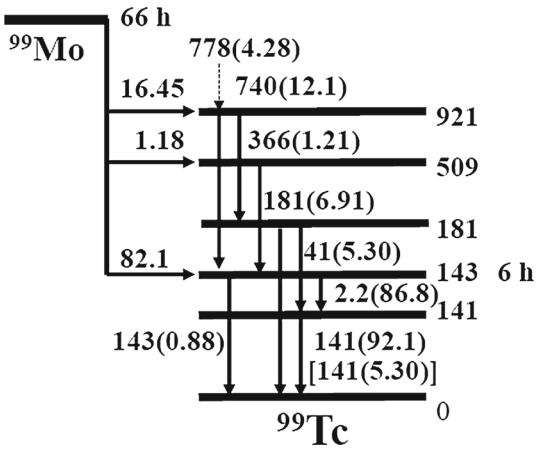

Fig. 1 A partial decay scheme of ^{99}Mo ($T_{1/2} = 66$ h) to excited states in ^{99}Tc. The half-life of ^{99m}Tc and ^{99}Tc is 6 h and 211,100 years, respectively

of ^{99}Mo is a key issue for ensuring the routine application of ^{99m}Tc. However, the supply chain of ^{99}Mo that is mostly produced by the fission reaction of ^{235}U in a limited number of research reactors operating over 50 years around the world is vulnerable since 2008 [9]. The vulnerable situation of the supply chain of ^{99}Mo is the impetus to study alternative methods for producing ^{99}Mo and/or ^{99m}Tc in reactors or accelerators [10].

2 ^{99}Tc in stars

2.1 Background

When we began our experimental study in nuclear astrophysics in 1989, using fast neutrons that were provided from an accelerator at the Tokyo Institute of Technology, there was great interest in the abundance of s-process isotopes for various metallicity stars in order to construct models of the chemical evolution of the Galaxy [11, 12]. Indeed, efforts involving observations and yields estimations of these s-process isotopes were being made for a wide range of metallicities and stellar masses to compare the chemical evolution models with the observational data [13]. In the models of the chemical evolution of the s-process isotopes for low-metallicity massive stars, it was necessary to clarify the relation between the yields of the s-process isotopes versus the abundance of ^{56}Fe (seed) nucleus and/or of ^{16}O (source) nucleus. In the weak s-process nucleosynthesis theory, neutrons from the ^{22}Ne(α,n)^{25} Mg reaction are used to produce s-process isotopes [14, 15]. Hence, if the neutron capture cross sections of abundant light nuclei, such as ^{12}C and ^{16}O, direct products of He burning, would be large, the yields of heavier s-process isotopes would decrease; the releationship of the yields versus the abundance of either ^{56}Fe and/or ^{16}O becomes nonlinear. Therefore, in order to construct a model that predicts s-process istope production as a function of metalllicity and stellar mass, it was necessary to know the neutron capture cross sections of these light nuclei at stellar neutron energy. However, these cross sections were rarely measured compared to the extensive measurements of capture cross sections of intermediate- and heavy-mass nuclei that were needed to interpret the various mechanisms of stellar nucleosynthesis [16, 17].

Based on the experimental status of neutron capture cross sections for light nuclei at that time, we challenged the measurement of neutron capture reaction cross sections for ^{12}C [18] and ^{16}O [19] at stellar neutron energies by combining a pulsed neutron beam and a prompt discrete γ-ray detection method. Among a variety of neutron sources [7], we used a pulsed neutron beam produced by the ^{7}Li(p,n)^{7}Be reaction in a small accelerator, as in the case of Franz Käppeler's Karlsruhe group at KfK. For the neutron capture γ-ray detection, our discrete γ-ray detection method was complementary to the detection method of the energy sum of the γ-ray cascade emitted in the decay of the compound nucleus, used in Karlsruhe and elsewhere. Here, it is worth-mentioning that the level density of excited states in light-mass isotopes that are populated by the keV-neutron capture reaction is low. We would therefore observe discrete γ rays emitted from the neutron capture states to the low-lying states of residual nucleus with specific spin-parity, excitation energies, and spectroscopic factors.

2.2 Experimental method: pulsed neutrons and discrete γ-ray detection

The pulsed neutrons were produced by the ^{7}Li(p,n)^{7}Be reaction at the 3.2-MV Pelletron Accelerator of the Research Laboratory for Nuclear Reactors at the Tokyo Institute of Technology [20]. Neutron energy spectra were measured by a ^{6}Li-glass scintillation detector by a time-of-flight (TOF) method. Discrete prompt γ rays emitted in the transition from a capture state of residual nucleus to low-lying states were measured by an anti-Compton NaI(Tl) spectrometer that was heavily shielded from backgrounds with ^{6}LiH, borated paraffin, Cd sheet, and Pb [18–20]. In this type of setup, background events could be due to γ rays from the ^{7}Li(p,γ)^{8}Be reaction, γ rays from the ^{127}I(n,γ)^{128}I reaction occurring in the NaI(Tl) spectrometer, γ and β rays from the decay of ^{128}I with $T_{1/2} = 25$ m, and γ rays from the decay of ambient natural radioactivity, such as ^{40} K and ^{208}Tl. Using the spectrometer together with the pulsed neutron beam we could measure discrete γ rays emitted after neutron capture reactions, even for small cross sections of about 10 μb at a neutron energy (E_n) of 30 keV. The relationship between a

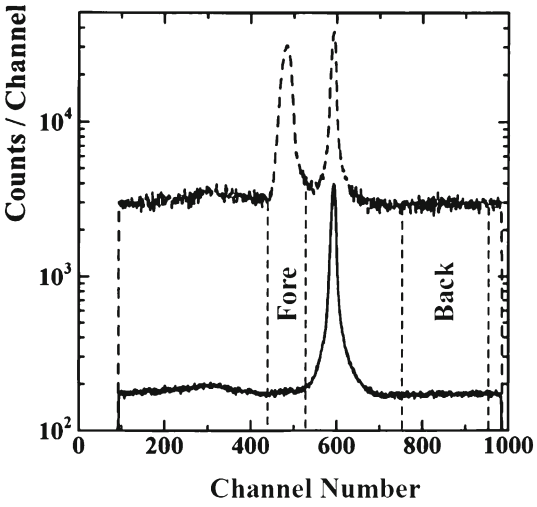

Fig. 2 Typical TOF spectrum for an Au sample used to normalize the absolute capture cross section of the $^{16}O(n,\gamma)^{17}O$ reaction at E_n = 398 keV taken by the NaI(Tl) spectrometer. Here, the dashed and solid lines indicate the TOF spectra for the Au and $^{2}H_2O$ samples, respectively

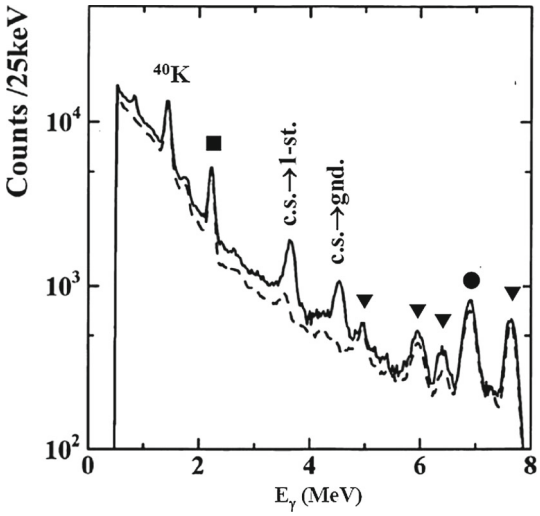

Fig. 3 γ-ray PH spectra from the $^{16}O(n,\gamma)^{17}O$ reaction at the neutron energy of 398 keV. Typical foreground and background spectra are respectively shown as solid and dashed lines. The background γ-ray peaks other than ^{40} K are from the $^{1}H(n,\gamma)^{2}H$ (filled square), $^{56}F(n,\gamma)^{57}Fe$ (down filled triangles), and $^{127}I(n,\gamma)^{128}I$ (filled circle) reactions

γ-ray pulse height (PH), taken by the central NaI(Tl) detector in the NaI(Tl) spectrometer, and neutron energy was determined by obtaining a TOF spectrum by using signals from the NaI(Tl) detector and the pulsed proton beams from the accelerator. The NaI(Tl) spectrometer was set at 125.3° with respect to the proton beam direction, where the second Legendre polynomial is zero and thus the γ-ray intensity measured at this angle provides the angle-integrated value for a dipole radiation emitted in the capture events. One set of each experimental run was composed of individual measurements for one of two oxygen compound samples of $^{7}Li_2O$ or $^{2}H_2O$, Au, and blank samples. Each experimental run was carried out by cyclically changing these samples to mitigate systematic uncertainties in the measurement. The blank run was performed to monitor any change in the primary neutron energy, to derive the thickness of the ^{nat}Li neutron production target during each set of experimental runs, and to determine the background without sample.

2.3 Experimental results

A typical TOF spectrum for an Au sample used to normalize the absolute capture cross section of the $^{16}O(n,\gamma)^{17}O$ reaction at E_n = 398 keV taken by the NaI(Tl) spectrometer is shown in Fig. 2 [21]. The sharp peak in channel 600 and the broad peak in channel 490 were attributed to the $^{7}Li(p,\gamma)^{8}Be$ and $^{197}Au(n,\gamma)^{198}Au$ reactions, respectively.

Typical foreground (Fore) and background (Back) PH spectra for the $^{16}O(n,\gamma)^{17}O$ reaction that were obtained by putting the gates on Fore- and Back-ground regions indicated in Fig. 2, are shown in Fig. 3. Note that, as shown in a net

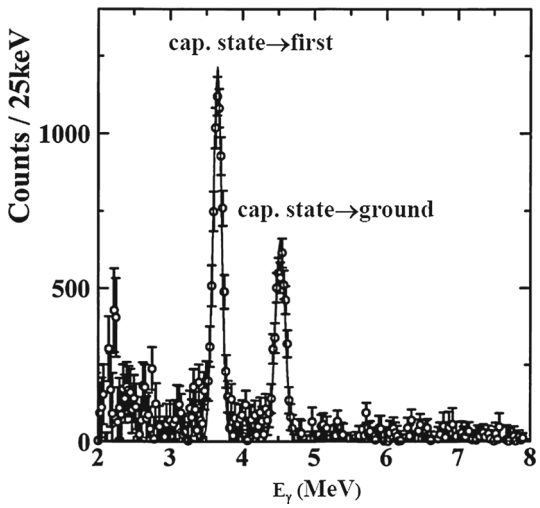

Fig. 4 Net γ-ray PH spectrum for the $^{16}O(n,\gamma)^{17}O$ reaction at the neutron energy of 468 keV

spectrum in Fig. 4, the discrete γ rays at 3.65 and 4.52 MeV corresponding to the γ rays emitted from the neutron capture state of ^{17}O to the first excited ($J^\pi = 1/2^+$) and the ground ($J^\pi = 5/2^+$) states of ^{17}O were clearly observed. The partial cross sections from the neutron capture state of ^{17}O to these lower-lying states of ^{17}O were determined by analyzing the intensities of these γ rays.

The γ-ray relative intensities thus obtained for 157 keV neutrons are compared with those generated by thermal neutrons [22] in Fig. 5. The γ-ray strength from the capture state of ^{17}O feeding directly to the first-excited state ($J^\pi = 1/2^+$)

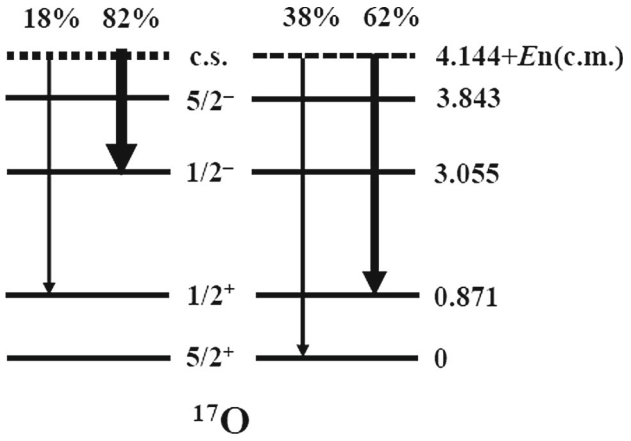

Fig. 5 γ-ray relative intensities for thermal neutrons (left) [22] are compared with those obtained by 157 keV neutrons (right) [21]

in ^{17}O is large for 157 keV neutrons, whereas the largest γ-ray strength is observed for the transition leading directly to the second-excited state ($J^{\pi} = 1/2^{-}$) for thermal neutrons. Since the thermal neutron capture proceeds only by *s*-wave neutrons, the strongest transition from the capture state of ^{17}O to the second-excited state is an E1 transition. Hence, assuming the same E1 character for the transition leading to the first-excited state ($J^{\pi} = 1/2^{+}$) also for 157 keV neutrons, the keV neutron capture process on ^{16}O was found to be dominated by a non-resonant direct *p*-wave capture process. Note that such a non-resonant direct *p*-wave neutron reaction process was also observed in the measurement of the ^{12}C(n,γ)^{13}C reaction cross sections at neutron energies from 10 to 530 keV [23].

By the way, the excited state of ^{17}O has a resonance state ($J^{\pi} = 3/2^{-}$) with the total width of about 40 keV at 4554 keV, corresponding to the neutron energy of 411 keV in the center-of-mass system. The resonance state can provide a great opportunity to study an interference between a non-resonant *p*-wave neutron capture process and a resonance neutron capture process in the ^{16}O(n,γ)^{17}O reaction in a relevant neutron energy region for astrophysical importance. Note that the excited state of ^{13}C populated by the ^{12}C(n,γ)^{13}C reaction at $E_n < 1$ MeV does not have such a resonance state. Hence, we extended the energy range of neutrons in the cross-section measurement of the ^{16}O(n,γ)^{17}O reaction at average neutron energies of 157, 349, 398, 427, 468, 498, and 556 keV to investigate the possibility of the aforementioned interference [21]. In the study, we prepared thin ^{nat}Li metal targets to cover the cross section measurements in the region of the $3/2^{-}$ resonance state with an energy resolution of about 50 keV full width at half maximum. Meanwhile, a thick ^{nat}Li metal target was used for the off-resonance region, because the cross section is considered to change smoothly with neutron energy.

Table 1 Measured partial and total cross sections of the ^{16}O(n,γ)^{17}O reaction

En (KeV)	σγ(c.s.→1st) [μb]	σγ(c.s.→g.s.) [μb]	σγ(total)[μb]
20	15.4(42)	6.0(35)	21.4(54)
40	20.1(28)	6.2(19)	26.3(33)
60	22.0(41)	7.5(29)	29.5(50)
157	21.6(21)	13.1(15)	34.7(28)
349	107(14)	54(10)	161(18)
398	177(14)	115(11)	292(16)
427	267(24)	146(13)	413(24)
468	25.1(23)	12.8(16)	37.9(28)
498	14.7(17)	4.6(9)	19.3(19)
556	28.6(22)	11.4(14)	40.0(26)

The data at $E_n = 20$, 40, and 60 keV are from Ref. [19]

The partial neutron capture cross section $\sigma_{\gamma,i}$, corresponding to the *i*-th γ-ray transition with energy $E_{\gamma,i}$ from the neutron capture state of ^{17}O to the low-lying state *i*, was obtained by using the γ-ray yield $Y_{\gamma,i}$ (^{17}O) as given in Eq. (1):

$$\sigma_{\gamma,i} = \frac{T_{\mathrm{O}}}{T_{\mathrm{Au}}}\frac{P_{\mathrm{Au}}}{P_{\mathrm{O}}}\frac{C_{\mathrm{Au}}}{C_{\mathrm{O}}}\frac{(r^2n)_{\mathrm{Au}}}{(r^2n)_{\mathrm{O}}}\frac{Y_{\gamma,i}(^{17}\mathrm{O})}{Y_{\gamma}(\mathrm{Au})}\sigma_{\gamma}(\mathrm{Au}) \quad (1)$$

Here, O and Au refer to ^{16}O and ^{197}Au, respectively. P_s and T_s are the number of the neutron counts measured by the ^{6}Li-glass detector and the neutron transmission of a sample s = {O, Au}, respectively. *r* and *n* are the radius and the thickness (atoms/barn) of sample s. Y_{γ}(Au) and σ_{γ}(Au) are the γ-ray yield and the absolute capture cross section for ^{197}Au, respectively. Y_{γ}(Au) and $Y_{\gamma,i}$(^{17}O) were obtained by using the response function of the NaI(Tl) spectrometer [24]. C_{Au} and C_{O} are correction factors for ^{197}Au and ^{16}O samples that are defined as the product of four factors. Namely, the factors to correct the γ-ray yield for multiple-scattering and self-shielding effects of the incident neutrons in the sample s, γ-ray absorption by the sample, and the finite size of the sample. Note that both the elastic and capture reaction processes were considered as main sources of neutron attenuation. The measured partial as well as the total cross sections of the ^{16}O(n,γ)^{17}O reaction are given in Table 1.

2.4 Conclusion

Model calculations of the (n,γ) cross section were performed to be compared with the measured results by using a theoretical approach based on a direct radiative capture (DRC) process coupled to a single-level Breit-Wigner (SLBW) resonance model [21, 25]. The results [21] are shown in Fig. 6,

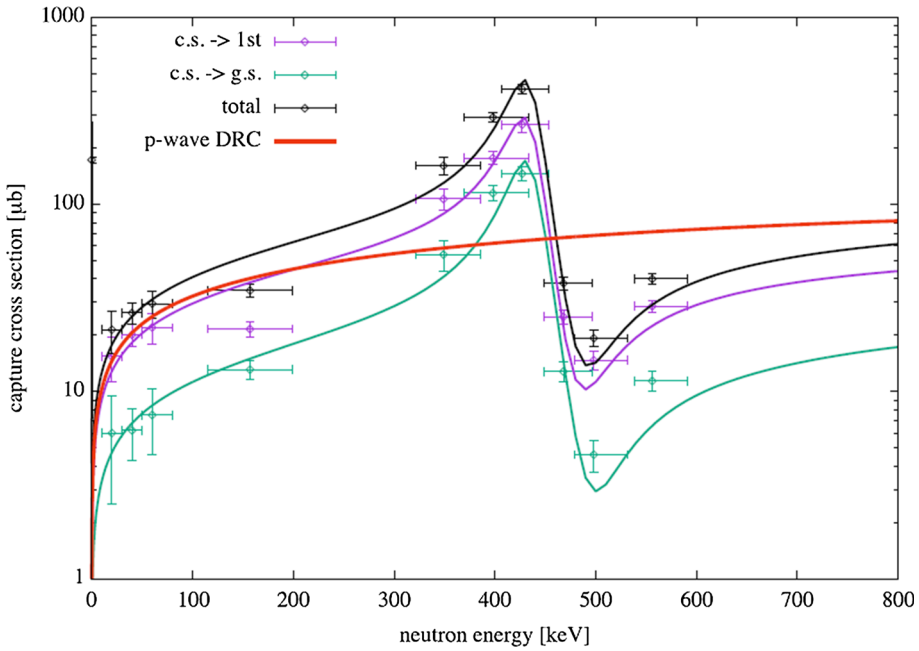

Fig. 6 Neutron capture cross section in the energy range up to 800 keV, fully covering the region of the *p*-wave resonance at 437 keV. The interference effect is clearly visible, for both transitions leading to the ground state as well as to the first-excited state in ^{17}O

where very good agreement is found between the model calculations and the present experimental results, both for the transitions leading to the ground state as well as for those leading to the first-excited state in ^{17}O. The interference effect is clearly visible, for both transitions leading to the ground state as well as to the first-excited state in ^{17}O.

Finally, a numerically integrated neutron capture reaction rate for the ^{16}O$(n,\gamma)^{17}$O reaction, $N_A < \sigma v >$, is calculated for the various components of the capture process, as given Eq. (2).

$$N_A < \sigma v > = a_0 + a_1 T_9 + a_2 / \left\{ (T_9)^{3/2} \right\} \times \exp(-2.225/T_9) \quad (2)$$

where σ is the Maxwellian-averaged capture cross section (MACS), T_9 is the temperature in 10^9 K. Here, the first term is determined by the thermal capture cross section, $\sigma_\gamma = 0.173 \pm 0.006$ mb [26], the second term is a good approximation of the *p*-wave DRC component, and the last term is the resonance term. The rate is in cm^3 s^{-1} mol^{-1} when the parameters are $a_0 = 26.5$ ($\pm$ 3.5%), $a_1 = 12{,}434$ (+ 10%−15%) and $a_2 = 56{,}820$ ($\pm$ 20%). In the present study, we confirmed that a non-resonant *p*-wave direct capture process plays a dominant role in the reaction at the neutron energy between 10 and about 300 keV. Furthermore, we found that the interference effect between the $3/2^-$ resonance state with the total width of 40 keV at $E_n = 411$ keV and a non-resonant *p*-wave direct contribution significantly dominates the reaction cross section at $E_n > 300$ keV. Based on the present results we determined the Maxwellian-averaged capture cross section for thermal energies between $kT = 5$ and 100 keV. Since we solved a longstanding problem of the ^{16}O$(n,\gamma)^{17}$O reaction cross section, we expect that the present results could contribute to the progress on the various astrophysical phenomena, as given in [27–30], as well as a neutron capture reaction process.

3 ^{99}Tc in reactors

3.1 Background

As aforementioned, ^{99g}Tc is one of the most important LLFPs for the study on the transmutation of nuclear wastes. However, experimental data for the capture cross sections of LLFPs are very poor both in quality and in quantity. As for ^{99g}Tc, there exist three sets [31–33] of capture cross sections in the keV region before starting the present study [34], but large discrepancies exist among the previous data.

One of the main reasons for the discrepant results is due to LLFP difficulties in sample preparation: it is not easy to prepare enough amount of high purity sample of LLFPs to perform ordinary keV neutron capture experiments. Another reason is due to the radioactivity of LLFP sample: the accurate measurement of capture γ rays from the radioactive sample is not easy. Therefore, we have developed a capture γ-ray spectrometer with high sensitivity [35] and it has become possible to perform the keV-neutron capture experiment with a small amount (less than 1 g) of sample.

3.2 Experimental procedure and data processing

The experimental procedure and data processing are briefly described, as follows. The capture cross sections of ^{99g}Tc were measured in the incident neutron energy region from 8 to 90 keV and at 190, 330, and 540 keV, using the same neutron source as that described in the previous section.

The ^{99g}Tc sample was oxide powder ($^{99g}TcO_2$) sealed in an aluminum case of the inner diameter of 20.0 mm. The net weight of ^{99g}Tc was 1.026 g (about 700 MBq) and the chemical purity of ^{99g}Tc was 99.6%. A ^{197}Au sample with a diameter of 20.0 mm and a thickness of 1.0 or 2.0 mm was used as a standard.

Capture γ rays were detected with a large anti-Compton NaI(Tl) spectrometer with a heavy shield [20] by means of TOF method. Capture events detected by the spectrometer were stored in a workstation as two-dimensional data of TOF and PH. On the other hand, the energy spectrum of neutrons incident on each sample was measured by a TOF method with a ^{6}Li-glass detector.

The measurements with and without the ^{99g}Tc sample, with the ^{197}Au sample, and with a ^{27}Al sample (corresponding to the aluminum case of the ^{99g}Tc sample) were made cyclically to average out changes in experimental conditions such as the incident neutron energy spectrum.

The γ-ray PH spectra for the ^{99g}Tc or ^{197}Au sample in the Fore- and Back-ground regions were extracted by analyzing the two-dimensional data of the γ-ray spectrometer. Then, the net capture γ-ray PH spectrum of the ^{99g}Tc or ^{197}Au sample was obtained by subtracting the Back-ground PH spectrum from the Fore-ground PH spectrum for each incident neutron energy spectrum.

A PH weighting technique [36] with the weighting function of the γ-ray spectrometer was applied to the net capture γ-ray PH spectra of the ^{99g}Tc and ^{197}Au samples to obtain the capture yields, i.e., the numbers of capture events. Finally, the capture cross section of ^{99g}Tc was derived by using the standard capture cross sections of ^{197}Au taken from ENDF/B-VI [37]. Corrections were made for the self-shielding and multiple-scattering of neutrons in the sample, the absorption and/or scattering of γ rays in the sample, the dead time, and others such as the effect of impurities in the ^{99g}Tc sample. In addition to the statistical error (1–4%), the following non-statistical errors were taken into account for those of capture cross sections: the errors due to the standard capture cross sections of ^{197}Au (3%), the weighting function of the γ-ray spectrometer (1%), the extrapolation of PH spectrum below the discrimination level of 0.6 MeV (2%), and the neutron self-shielding and multiple-scattering correction factors (1–2%). The total uncertainty of about 5% was evaluated by taking the square root of a quadratic sum of the statistical and nonstatistical errors.

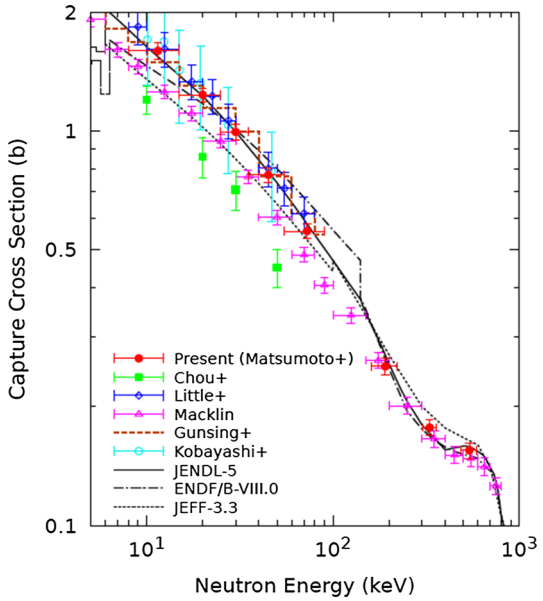

Fig. 7 Neutron capture cross sections of ^{99g}Tc in the keV region. Previous measurements and recent evaluated values are also shown

3.3 Results and discussion

The capture cross sections of ^{99g}Tc were derived with the error of about 5% in the neutron energy region from 8 to 90 keV and at 190, 330, and 540 keV. The present results are shown in Fig. 7, and compared with other measurements [31–33, 38, 39] and the evaluated values in JENDL-5 [40], ENDF/B-VIII.0 [41], and JEFF-3.3 [42].

Chou and Werle [31] measured the capture cross sections in the neutron energy region from 1 eV to 50 keV, using a lead slowing-down spectrometer with a 14 MeV neutron source at Karlsruhe. Their results from 10 to 50 keV are smaller than the present ones by about 30%. Little and Block [32] measured the capture cross sections up to 80 keV, using a photo-neutron source by the electron linear accelerator of the Rensselaer Polytechnic Institute. Their results from 10 to 80 keV agree with the present ones within the experimental errors. Macklin [33] measured the capture cross sections in the energy region of 2.65 to 2000 keV, using the Oak Ridge Electron Linear Accelerator (ORELA). His results from 10 to 80 keV are smaller than the present ones by 15–20%, but his results from about 150–600 keV are in good agreement with the present ones. After starting the present measurements, Gunsing et al. [38] reported their results from 3 to 90 keV, which were obtained from the measurement with the pulsed white neutron source GELINA at Geel. Their results seem to support the present results, although they did not give the errors of their results. Kobayashi et al. [39] measured the capture cross sections in the energy region of 0.005 eV to 47 keV, using the 46-MeV electron linear accelerator at the

Kyoto University, Research Reactor Institute. Their results above 10 keV are in good agreement with the present ones.

The evaluated values of JENDL-5 are in excellent agreement with the present measurements in the whole energy region. The evaluations of ENDF/B-VIII.0 around 10 keV are smaller than the present result at 12 keV by about 10%, but the evaluations around 70 keV are larger than the present result at 69 keV by about 15%. Namely, the energy dependence of ENDF/B-VIII.0 evaluations is gentle compared to that of the present measurements in the neutron energy region from about 10 to 100 keV. On the other hand, above 190 keV, the ENDF/B-VIII.0 evaluations are in good agreement with the present measurements. As for the evaluations of JEFF-3.3, those below 70 keV are smaller than the present results by 5−20%, but those above 190 keV are larger than the present results by 5−10%.

3.4 Conclusion

The capture cross sections of ^{99g}Tc were measured in the incident neutron energy region from 8 to 90 keV and at 190, 330, and 540 keV, using a 1.5 ns pulsed neutron source by the ^{7}Li(p,n)^{7}Be reaction and a large anti-Compton NaI(Tl) γ-ray spectrometer. The errors of the present capture cross sections were about 5%. In the 8–90 keV region, the present measurements were larger than those of Macklin by 15–20% and those of Chou and Werle by about 30%, but agreed with those of Little and Block, those of Gunsing et al. and those of Kobayashi et al. On the other hand, the present results at 190, 330, and 540 keV were in good agreement with those of Macklin. The present accurate data on the neutron capture cross sections of ^{99g}Tc that were obtained using an unconventional and unique experimental method also contribute to improve its evaluated cross sections, as shown below. The evaluations of JENDL-5 were in excellent agreement with the present results. On the other hand, there existed discrepancies between the present results and the evaluations of ENDF/B-VIII.0 and JEFF-3.3.

4 ^{99m}Tc in nuclear medicine

4.1 Background

Medical radioisotopes (RIs) have been used for diagnostic imaging studies of diseases and therapeutic applications in cancer treatments [43]. Among the medical RIs, ^{99m}Tc ($T_{1/2}$ = 6 h), the decay product of ^{99}Mo ($T_{1/2}$ = 66 h), is the most widely used diagnostic nuclear medicine RI that is usually obtained from a ^{99}Mo/^{99m}Tc generator [8]. Because of the short half-life of ^{99}Mo a constant supply of ^{99}Mo is a key issue for ensuring

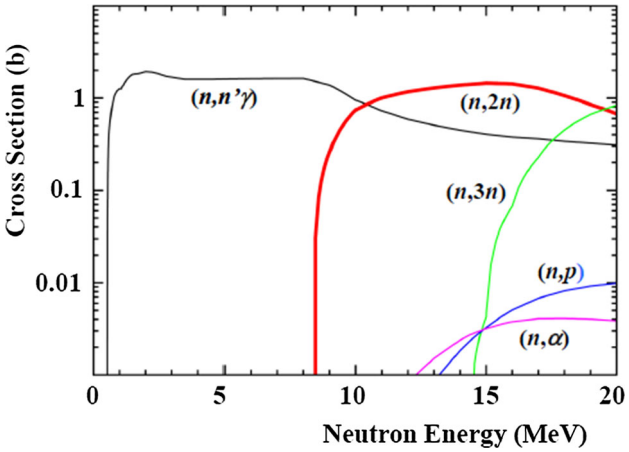

Fig. 8 Neutron-induced reaction cross sections on.^{100}Mo [46]

the routine application of ^{99m}Tc. Typical proposed reactions are the ^{98}Mo(n,γ)^{99}Mo reaction in reactors and the ^{100}Mo(p,pn)^{99}Mo, ^{100}Mo(p,2n)^{99m}Tc, ^{235}U(n,fission)^{99}Mo, ^{238}U(γ,fission)^{99}Mo, and ^{100}Mo(γ,n)^{99}Mo reactions in accelerators [10]. Here, it should be mentioned that all alternative ^{99}Mo production routes would face the challenges of lower reaction rates and lower specific activity. In fact, the current route of fission-^{99}Mo provides a large amount of ^{99}Mo with a high specific activity of ~ 370 TBq/(g ^{99}Mo) in a reactor. On the other hand, a specific activity of ^{99}Mo based on any alternative routes, other than that of fission-^{99}Mo, is as low as about 1/5000 of the fission-^{99}Mo production [44].

In 2009, we proposed a new route to produce ^{99}Mo by the ^{100}Mo(n,2n)^{99}Mo reaction using fast neutrons from an accelerator (Hereinafter referred to as accelerator neutrons) [45]. Here, we discuss important physical parameters in the ^{100}Mo(n,2n)^{99}Mo reaction to produce a large amount of ^{99}Mo that can mitigate the aforementioned challenges. They are the cross section of the reaction, accelerator neutron beam flux, and number of ^{100}Mo sample nuclei. Firstly, that cross section has been evaluated based on the measurement and is as large as about 1.5 barn in the neutron energy (E_n) range between 12 and 20 MeV, as shown in Fig. 8 [46]. On the other hand, the cross sections of the ^{100}Mo(n,α), ^{100}Mo(n,3n), and ^{100}Mo(n,p) reactions that produce impurity radioisotopes other than ^{99}Mo are less than a few mb at E_n ~ 14 MeV. Hence, we could expect to obtain a high radionuclide purity of ^{99}Mo. Secondly, an intense accelerator neutron flux of 10^{15} n/s that has a most probable E_n of 14 MeV is produced by the ^{nat}C(d,n) reaction using 40 MeV, 5 mA deuterons [47]. The neutron spectrum is advantageous for producing ^{99}Mo (see Fig. 8). The neutrons are mostly emitted in the forward-direction with respect to the deuteron beam direction. Hence, a ^{100}Mo sample placed at the forward-direction is effectively irradiated with the neutrons to produce ^{99}Mo. A quantity of ^{100}Mo samples of over 100 g mass can be used, because the

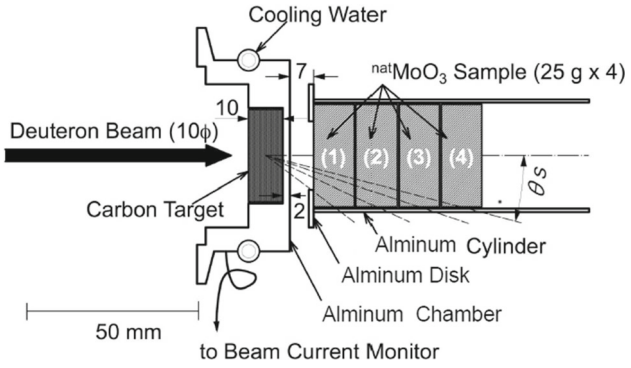

Fig. 9 Schematic view of the experimental setup at the $^{nat}MoO_3$ sample position. Sample numbers are indicated in parentheses. [48]

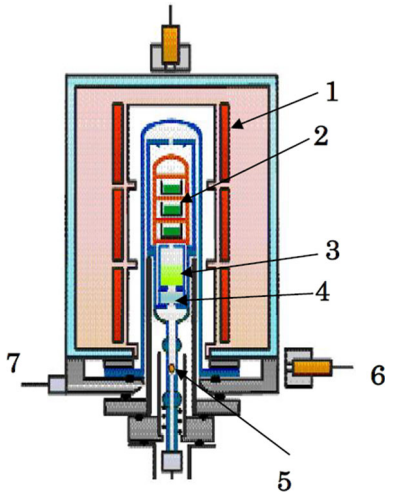

Fig. 10 Schematic view of thermochromatography system. 1, Electric furnace (three individual heating zones); 2, Crucibles for MoO_3 samples; 3, MoO_3 needle crystal holder; 4, Quartz wool; 5, ^{99m}Tc condensation region; 6, CZT detector; 7, Moist oxygen inlet

neutron has no charge, and therefore the traveling range in a sample is much longer than that of a charged particle that is demonstrated in the measurement of the ^{99}Mo yield using a thick ^{nat}Mo sample in the next section.

4.2 ^{99}Mo yield studied by using neutrons from the C(d,n) reaction

Next, in order to estimate an available production yield of ^{99}Mo on the basis of the proposed route we made a rigorous test of the measured energy and angular distributions of the accelerator neutrons, including the evaluated cross section of the ^{100}Mo(n,2n)^{99}Mo reaction. The test was made by measuring the yield of ^{99}Mo produced by the ^{nat}Mo(n,2n)^{99}Mo reaction [48]. We used four pellet $^{nat}MoO_3$ samples of 25.869, 25.868, 25.483 and 25.220 g mass with dimensions of 30 mmϕ × 11.6 mm (total length 46.4 mm), as shown in Fig. 9. The accelerator neutrons were provided by the ^{nat}C(d,n) reaction using 40 MeV deuterons at the cyclotron at Cyclotron and Radioisotope Center (CYRIC), Tohoku University [49].

We estimated the yield of ^{99}Mo by numerical calculations for a comparison with the measured yield, as follows. We used the neutron-nucleus reaction cross sections given in JENDL-4.0 [46] for molybdenum and oxygen in the $^{nat}MoO_3$ sample. In calculating the neutron flux we used the latest data of the cross section, which was obtained by irradiating a 15-mm-thick carbon target with 40 MeV deuteron beams [50]. The estimated yield of ^{99}Mo for each set of the ^{nat}Mo samples is in good agreement with the measured yield, as given in Table 2.

Based on the good agreement between the measured ^{99}Mo yield and the calculated yield, we calculated the activities of ^{99}Mo at the end of irradiation (EOI), produced by the ^{100}Mo(n,2n)^{99}Mo reaction for an enriched $^{100}MoO_3$ sample. In the calculation, we used the latest data on the angular and energy distributions of neutrons from ^{nat}C(d,n) at E_d = 40 MeV (assuming a beam intensity of 2 mA) and evaluated cross sections given in JENDL-4.0. We obtained the calculated yield of 700 GBq ^{99}Mo using a $^{100}MoO_3$ sample of 100 g produced every day by the ^{100}Mo(n,2n)^{99}Mo reaction with 40 MeV, 2 mA deuteron beams (24 h irradiation) [48]. If 700 GBq of ^{99}Mo is produced daily, 6 days a week, the daily production of ^{99}Mo is stockpiled, so that an average of 2.44 TBq of ^{99}Mo per day [48] is used to obtain ^{99m}Tc, which is discussed in subsection 4.3. A detailed discussion of average ^{99}Mo yields can be found in Ref. 51 (Fig. 3).

4.3 Thermoseparation of ^{99m}Tc from ^{99}Mo with a low specific activity

First, it should be noted that the typical radioactivity of ^{99m}Tc radiopharmaceutical solutions administered to patients is as high as about 740 MBq/(several ml). In order to recover ^{99m}Tc with such high specific activity from ^{99}Mo with aforementioned low specific activity, various method, such as chromatographic, solvent extraction, and thermoseparation methods, have been developed.

We employed the thermoseparation procedure, which utilizes the different volatility of technetium oxide and $^{100}MoO_3$ to separate ^{99m}Tc from ^{99}Mo. We developed newly a homemade thermochromatography system shown in Fig. 10 to achieve a higher separation efficiency of ^{99m}Tc over 90% for an irradiated $^{100}MoO_3$ sample of about 100 g [52], a high capability of nearly 100% recovery of irradiated enriched $^{100}MoO_3$ sample [53]. Note that it is important to recycle an enriched (expensive) ^{100}Mo sample irradiated by neutrons.

The ^{99m}Tc activity that can be obtained from the aforementioned 2.44 TBq ^{99}Mo using the thermochromatography system was evaluated as follows. First, the irradiated

Table 2 Measured ^{99}Mo yield ($^{99}Mo_{meas.}$) at the EOI compared with the calculated yield ($^{99}Mo_{cal.}$). The number in brackets in the first line is the number of the sample shown in Fig. 9

$^{nat}MoO_3$ (g)	25.869 (1)	25.868 (2)	25.483 (3)	25.220 (4)
$^{99}Mo_{meas.}$(10^4 Bq)	3.9 ± 0.2	2.6 ± 0.1	1.7 ± 0.1	1.3 ± 0.1
$^{99}Mo_{cal.}$(10^4 Bq)	3.6 ± 0.7	2.3 ± 0.4	1.5 ± 0.3	1.0 ± 0.2

$^{100}MoO_3$ sample containing the ^{99}Mo is placed in a thermochromatography apparatus to separate ^{99m}Tc twice a day from the ^{99}Mo. The ^{99m}Tc activity immediately after separating ^{99m}Tc from the ^{99}Mo was evaluated to be 2.35 TBq in which the separation efficiency of 80% and the decay loss of ^{99m}Tc during the separation procedure for about 2 h were considered.

Next, quality control testing of ^{99m}Tc-radiopharmaceuticals using the ^{99m}Tc thus obtained is described. Note that the current United States Pharmacopeia (USP) contains regulatory requirements concerning the radionuclidc purity and the radiochemical purity of ^{99m}Tc. The USP sets those pharmacopeia standards for $^{99m}TcO_4^-$ obtained from a ^{99}Mo/^{99m}Tc generator. We have tested the pharmaceutical equivalence of $^{99m}TcO_4^-$ obtained by ^{99m}Tc from the thermochromatographic separation procedure to that obtained from the alumina-based ^{99}Mo/^{99m}Tc generator. We have also studied quality-control tests of ^{99m}Tc-radiopharmaceuticals commonly used for the imaging of brain perfusion (^{99m}Tc-ECD), myocardial perfusion (^{99m}Tc-MIBI), and kidney (^{99m}Tc-MAG3), to ensure the safe clinical use of ^{99m}Tc obtained by the ^{100}Mo(n,2n)^{99}Mo reaction. The results of the quality assessments of the $^{99m}TcO_4^-$ saline solution and ^{99m}Tc-radiopharmaceuticals were shown to satisfy the USP requirements. These results provide the important evidence that ^{99m}Tc prepared by thermochromatographic separation using ^{99}Mo produced by the ^{100}Mo(n,2n)^{99}Mo reaction can be a promising substitute for the fission product ^{99}Mo [52].

4.4 ^{99}Mo demand in Japan and conclusion

Next, we will examine the extent to which 2.35 GBq of ^{99m}Tc can be covered in the nuclear medicine diagnosis of ^{99m}Tc performed in Japan. About 0.9 million diagnostic procedures (2750 procedures/day) have been performed every year using ^{99m}Tc radiopharmaceuticals with an average dose of about 740 MBq (20 mCi) at the time of injection to a patient: 2.05 TBq (55 Ci) of ^{99m}Tc is used every day. By considering the decay losses associated with transporting ^{99m}Tc from radiopharmaceutical companies to hospitals, a total of 4.10 TBq (110 Ci) of ^{99m}Tc is needed daily in Japan [48]. As discussed above, 2.35 TBq of ^{99m}Tc is obtained at the end of the separation of ^{99m}Tc, i.e., immediately before forming the ^{99m}Tc radiopharmaceuticals at a radiopharmaceutical company. When one can inject the ^{99m}Tc radiopharmaceuticals prepared by using the 2.35 TBq ^{99m}Tc within 6 h to a patient, about 57% of the daily procedures using ^{99m}Tc radiopharmaceuticals can be performed in Japan. In fact, because about 35% of Japan's population live in the capital-area (a region within about 150 km radius from the center of Tokyo), and the number of people who live in the capital-area, Kansai-area, and Chukyo-area is about 60% of the total population of Japan, ^{99m}Tc radiopharmaceuticals can be delivered from a radiopharmaceutical company to those who live there within 6 h. The proposed delivery of ^{99m}Tc would be possible by using the current delivery system of ^{18}F-FDG, a radiopharmaceutical fluorodeoxyglucose containing ^{18}F with a half-life of 1.8 h, shorter than ^{99m}Tc ($T_{1/2} = 6$ h). In Japan, deliveries of ^{18}F-FDG are being carried out three times per day by road transport from the ^{18}F-FDG-producing radiopharmaceutical company to hospitals about 200 km away within 3 h [54]. The activity of ^{18}F prepared at the radiopharmaceutical company is three times stronger than that needed for the injection into a patient at the hospital by considering the decay loss of 68% during the transportation of ^{18}F in 3 h. Note that the ^{99m}Tc activity needed at hospitals for the ^{99m}Tc procedures to satisfy 50% of the demand in Japan is 1.03 TBq (28 Ci). The decay loss of ^{99m}Tc activity in transportation for 3 h is 30%. Hence, the ^{99m}Tc activity of 2.35 TBq (64 Ci) obtained at a radiopharmaceutical company would be enough to perform the procedures mentioned.

Based on these results and the results of the quality assessment of ^{99m}Tc radiopharmaceuticals, it can be concluded that ^{99}Mo produced by the ^{100}Mo(n,2n)^{99}Mo reaction is a promising alternative to fission-^{99}Mo for domestic use [52].

5 Summary

The discovery of ^{99}Tc has opened up new research area, s-process nucleosynthesis in stars, nuclear transmutation of long-lived nuclear waste produced in fission reactors, and diagnosis in nuclear medicine, that were unforeseen at the time of its discovery. The present paper summarizes the results of our studies on ^{99g}Tc and ^{99m}Tc using

an accelerator-based neutron source that have been performed based on either by developing a neutron time-of-flight method combined with a discrete γ-ray detection technique using an anti-Compton NaI(Tl) spectrometer having high sensitivity or by proposing a new production scheme of medical radioisotope of ^{99m}Tc. A non-resonant p-wave direct capture process observed in the $^{16}O(n,\gamma)^{17}O$ reaction is shown to play a dominant role in the reaction at the neutron energy between 10 and about 300 keV, and in addition the interference effect between the $3/2^-$ resonance state in ^{17}O at $E_n = 411$ keV and a non-resonant p-wave direct contribution significantly dominates the reaction cross section at $E_n > 300$ keV. The resulting Maxwellian-averaged capture cross section for thermal energies between $kT = 5$ and 100 keV is expected to contribute to the progress on the various astrophysical phenomena as well as a neutron capture reaction process. The capture cross sections of ^{99g}Tc were measured in the incident neutron energy region between 8 and 540 keV accurately with an uncertainty of about 5% that provides valuable information on the nuclear transmutation of ^{99g}Tc and the s-process nucleosynthesis. The quality assessments of ^{99m}Tc-radiopharmaceuticals prepared using ^{99}Mo produced by the $^{100}Mo(n,2n)^{99}$Mo reaction were shown to satisfy the quality control test of USP requirements that can be a promising substitute for the fission product ^{99}Mo for domestic use. We are pleased to have been involved in different aspects of the ^{99}Tc research activities, pioneered by our colleague and friend Franz Käppeler and to have made the contributions described here.

Acknowledgements We would like to thank to Alberto Mengoni for carefully reading and giving critical comments on this manuscript and Nobuyuki Iwamoto for useful discussions. The present work was supported by JSPS KAKENHI Grant Number JP19K03903, and in part by Program on Open Innovation Platform with Enterprises, Research Institute and Academia, Japan Science and Technology Agency (JST, OPERA, JPMJOP1721).

Data availability statement This manuscript has no associated data or the data will not be deposited. [Authors' comment: The datasets generated and/or analyzed during the current study are available from the corresponding author on reasonable request.]

References

1. C. Perrier, E. Segré, J. Chem. Phys. **5**, 712 (1937)
2. E.O. Lawrence, N.E. Edelfson, Science **72**, 376 (1930)
3. E. Segré, G.T. Seaborg, Phys. Rev. **54**, 772 (1938)
4. R. B. Firestone, L. P. Ekström, Table of Radioactive Isotopes, Version 2.1, available on http://ie.lbl.gov/toi/index.asp. (2004)
5. P.W. Merrill, ApJ. **116**, 21 (1952)
6. S. Little, I. Little-Marenin, W. Bauer, Astronom. J. **94**, 981 (1987)
7. F. Käppeler, R. Gallino, S. Bisterzo, W. Aoki, Rev. Mod. Phys. **83**, 157 (2011)
8. C.S. Cutler, H.M. Hennkens, S. Sisay, S. Huclier-Markai, S.S. Jurisson, Chem. Rev. **113**, 858 (2013)
9. T. Ruth, Nature **457**, 536 (2009)
10. K. Bertsche, Proceedings of IPAC'10, Kyoto, Japan, 121 (2010)
11. R. Gallino, M. Busso, G. Picchio, C.M. Raiteri, A. Renzini, ApJ **334**, L45 (1988)
12. J.C. Wheeler, C. Sneden, J.W. Truran, ARA & A **27**, 279 (1989)
13. N. Prantzos, M. Hashimoto, K. Nomoto, A & A **234**, 211 (1990)
14. J. W. Truran, I. Jr. Iben, ApJ, **216**, 797 (1977)
15. M. Busso, R. Gallino, A&A **151**, 205 (1985)
16. R.L. Macklin, J.H. Gibbons, Rev. Mod. Phys. **37**, 166 (1965)
17. F. Käppeler, H. Beer, K. Wisshak, Rep. Prog. Phys. **52**, 945 (1989)
18. Y. Nagai, M. Igashira, K. Takeda, N. Mukai, S. Motoyama, F. Uesawa, H. Kitazawa, T. Fukuda, ApJ **372**, 683 (1991)
19. M. Igashira, Y. Nagai, K. Masuda, T. Ohsaki, H. Kitazawa, ApJ **441**, L89 (1995)
20. M. Igashira, H. Kitazawa, N. Yamamuro, Nucl. Instr. Meth. **A245**, 432 (1986)
21. Y. Nagai, M. Kinoshita, M. Igashira, Y. Nobuhara, H. Makii, K. Mishima, T. Shima, A. Mengoni, Phys. Rev. C **102**, 044616 (2020)
22. A. McDonald, E. Earle, M. Lone, F. Khanna, H. Lee, Nucl. Phys. A **281**, 325 (1977)
23. T. Kikuchi, Y. Nagai, T.S. Suzuki, T. Shima, T. Kii, M. Igashira, A. Mengoni, T. Otsuka, Phys. Rev. C **57**, 2724 (1998)
24. S. Mizuno, M. Igashira, K. Masuda, J. Nucl. Sci. Technol. (Abingdon, U.K.) **36**, 493 (1999)
25. P. Mohr, C. Heinz, M. Pignatari, I. Dillmann, A. Mengoni, F. Käppeler, ApJ **827**, 29 (2016)
26. Atlas of Neutron Resonances, edited by S. Mughabghab, 6th ed. (Elsevier, Amsterdam, 2018), p. 122
27. M. Rayet, M. Hashimoto, Astron. Astrophys. **354**, 740 (2000)
28. S.E. Woosley, A. Heger, T.A. Weaver, Rev. Mod. Phys. **74**, 1015 (2002)
29. L. S. The, M. F. El. Eid, B. S. Meyer, ApJ, **655**, 1058 (2007)
30. M. He, S.S. Zhang, M. Kusakabe, S. Xu, T. Kajino, ApJ **899**, 133 (2020)
31. J.C. Chou, H. Werle, J. Nucl. Energy **27**, 811 (1973)
32. R.C. Little, R.C. Block, Trans. Am. Nucl. Soc. **26**, 574 (1977)
33. R.L. Macklin, Nucl. Sci. Eng. **81**, 520 (1982)
34. T. Matsumoto, M. Igashira, T. Ohsaki, J. Nucl. Sci. Technol. **40**, 61 (2003)
35. M. Igashira, K. Tanaka, K. Masuda, Proc. 8th Int. Symp. on Capture Gamma-Ray Spectroscopy and Related Topics, Fribourg, Switzerland, Sept. 20–24, 1993, (edited by J. Kern), World Scientific, Singapore, 992 (1994)
36. R.L. Macklin, J.H. Gibbons, Phys. Rev. **159**, 1007 (1967)
37. ENDF/B-VI data file for 197Au (MAT=7925), evaluated by P. G. Young, (1991)
38. F. Gunsing, A. Lepretre, C. Mounier, C. Raepsaet, C. Bastian, F. Corvi, J. Gonzalez, Nucl. Phys. A **688**, 496c (2001)
39. K. Kobayashi, S. Lee, S. Yamamoto, T. Kawano, Nucl. Sci. Eng. **146**, 209 (2004)

40. O. Iwamoto, N. Iwamoto, K. Shibata, A. Ichihara, S. Kunieda, F. Minato, S. Nakayama, "Status of JENDL", EPJ Web of Conferences, vol.239, 09002_1–6 (2020); O. Iwamoto, N. Iwamoto, S. Kunieda et al., "Japanese Evaluated Nuclear Data Library version 5: JENDL-5", s ubmitted to Journal of Nuclear Science and Technology
41. D. Brown, M. Chadwick, R. Capote et al., ENDF/B-VIII.0: The 8th major release of the nuclear reaction data library with CIELO-project cross sections, new standards and thermal scattering data. Nucl. Data Sheets **148**, 1 (2018)
42. A. J. M. Plompen, O. Cabellos, C. De Saint Jean, et al. "The joint evaluated fission and fusion nuclear data library, JEFF-3.3", Euro Phys J A, **56**, 181 (2020)
43. International atomic energy agency, Vienna 2004, Nucl Technol Rev 62 (2004)
44. A. Dash, Jr., F. F. (Russ) Knapp, M. R. A. Pillai, Nuclear Medicine and Biology, **40**, 167 (2013)
45. Y. Nagai, Y. Hatsukawa, J. Phys. Soc. Jpn. **78**, 033201–033211 (2009)
46. K. Shibata, O. Iwamoto, T. Nakagawa, N. Iwamoto, A. Ichihara, S. Kunieda, S. Chiba, K. Furutaka, N. Otuka, T. Ohsawa, T. Murata, H. Matsunobu, A. Zukeran, S. Kamada, J. Katakura, J. Nucl. Sci. Technol. **48**, 1 (2011)
47. M. Fadil, B. Rannou, the SPIRAL2 project team. Nucl. Instr. Meth. B **266**, 4318 (2008)
48. K. Tsukada, Y. Nagai, K. Hashimoto, M. Kawabata, F. Minato, H. Saeki, S. Motoishi, M. Itoh, J. Phys. Soc. Jpn. **87**, 043201–043211 (2018)
49. M. Fujita, A. Terakawa, H. Suzuki, T. Endo, A. Yamazaki, E. Tanaka, T. Miyake, M. Tanigaki, H. Orihara, M. Fujioka, H. Okamura, and T. Shinozuka, Proceedings of The 17th International Conference on Cyclotrons and Their Applications. Tokyo, 143 (2004)
50. G. Lhersonneau, T. Malkiewicz, K. Kolos, M. Fadil, H. Kettunen, M.G. Saint-Laurent, A. Pichard, W.H. Trzaska, G. Tyurin, L. Cousin, Nucl. Instr. Meth. A **603**, 228 (2009)
51. F. Minato, K. Tsukada, N. Sato, S. Watanabe, H. Saeki, M. Kawabata, S. Hashimoto, Y. Nagai, J. Phys. Soc. Jpn. **86**, 114803–114811 (2017)
52. Y. Nagai, Y. Nakahara, M. Kawabata, Y. Hatsukawa, K. Hashimoto, H. Saeki, S. Motoishi, A. Ohta, T. Shiina, Y. Kawauchi, J. Phys. Soc. Jpn. **86**, 053202–053211 (2017)
53. M. Kawabata, S. Motoishi, H. Saeki, K. Hashimoto, Y. Nagai, J. Phys. Soc. Jpn. **86**, 053201–053211 (2017)
54. T. Fujiwara, Delivery PET Fundamental and Clinical Studies (April 2013) [in Japanese]